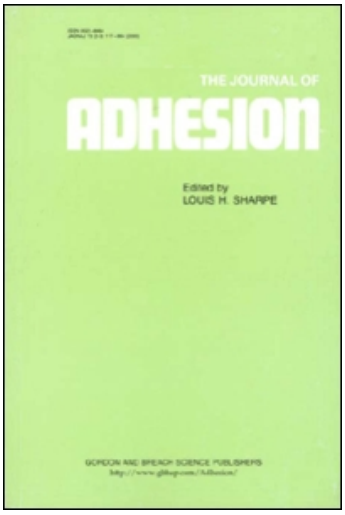

The Journal of Adhesion
Publication details, including instructions for authors and subscription information:
http://www.informaworld.com/smpp/title~content=t713453635

Local Dynamics of Adhesives in Aggressive Environment in the *Pre-Damage* Stage

Jovan Mijovic[a]; Nobuhiro Miura[a]; Som Soni[b]
[a] Department of Chemical Engineering and Chemistry and The Herman F. Mark Polymer Research Institute, Polytechnic University, Brooklyn, NY, USA [b] AdTech Systems Research, Beavercreek, OH, USA

To cite this Article Mijovic, Jovan , Miura, Nobuhiro and Soni, Som(2001) 'Local Dynamics of Adhesives in Aggressive Environment in the *Pre-Damage* Stage', The Journal of Adhesion, 76: 2, 123 — 150
To link to this Article: DOI: 10.1080/00218460108029621
URL: http://dx.doi.org/10.1080/00218460108029621

J. Adhesion, 2001, Vol. 76, pp. 123–150
Reprints available directly from the publisher
Photocopying permitted by license only

Local Dynamics of Adhesives in Aggressive Environment in the *Pre-Damage* Stage

JOVAN MIJOVIC[a,*], NOBUHIRO MIURA[a] and SOM SONI[b]

[a]*Department of Chemical Engineering and Chemistry and The Herman F. Mark Polymer Research Institute, Polytechnic University, Six MetroTech Center, Brooklyn, NY 11201, USA;* [b]*AdTech Systems Research, 1342 N. Fairfield Road, Beavercreek, OH 45432, USA*

(Received 29 September 2000; In final form 9 January 2001)

Molecular aspects of chemical and physical changes in adhesive joints caused by absorbed moisture were investigated. The focus was on the pre-damage stage that precedes the formation of voids and microcracks. A model and a commercial epoxy-amine formulation were studied. Local dynamics were monitored by broad-band dielectric relaxation spectroscopy (DRS). One portion of the absorbed water does not form hydrogen bonds with the network and gives rise to a fast relaxation process (termed γ) with activation energy of 28 kJ/mol. The local β dynamics are slowed down by the interactions between water and various sites on the network that include the ether oxygen, the hydroxyl group and the tertiary amine nitrogen. One particularly significant finding is that the average relaxation time for the β process above 20°C is of the order of nanoseconds or less and, hence, the detection and monitoring of this process hinges upon the ability to perform high-precision DRS at frequencies above 1 MHz. This is an important consideration in the ongoing efforts aimed at the implementation of DRS as non-destructive inspection (NDI) tool for adhesive joints.

Keywords: Adhesive; Environmental exposure; Dielectric relaxation spectroscopy; Local dynamics

*Corresponding author. Tel.: 718-260-3097, Fax: 718-260-3125, e-mail: jmijovic@poly.edu

INTRODUCTION

The continuing under-utilization of adhesive joints (particularly in aerospace structures) is widely recognized despite their advantages over riveted joints in terms of weight savings, structural integrity and design flexibility. There is little doubt that this problem stems largely from insufficient fundamental understanding of the effect of environment on adhesive joints. As a result, a strong initiative has emerged in recent years [1] aimed at identifying and monitoring changes in chemical and physical properties of adhesives at a *molecular level* from the very beginning of exposure to environment. The consensus of opinion is that this early, *pre-damage* stage (that precedes the formation of voids and microcracks that lead to the degradation of joints) holds the key to the understanding of initiation, propagation and failure.

The *chemical and physical* changes in adhesive joints in service occur at a rate that depends on the type and severity of the aggressive environment (we use term "aggressive" to stress that every environment will have an effect on the bondline, though on a different time scale). *Chemical* changes relate to the chemical state of the matter, as defined by the composition and chemical interactions (*e.g.*, complex formation, hydrogen bonding), while *physical* changes encompass the variations in molecular motions and mobility, relaxation dynamics, *etc.* The majority of the studies reported hitherto, however, have been concerned with the effect of moisture on *macroscopic* (bulk) properties and the detection of delamination and loss of adhesion that occur when water eventually diffuses through the adhesive and reaches the adhesive/adherend interface/interphase [2 – 12]. Our interest focuses on the *molecular events* in glassy adhesives in the pre-damage stage, where numerous fundamental questions remain unanswered. In what form (single molecules, dimers, trimers, complexes) does the absorbed water reside in the adhesive? How does water interact with the host matrix and what effect does that have on the local dynamics? What are the effects of the temperature, pressure and relative humidity of the environment? It is expected that the knowledge gained in this study will usher workers along the way for the development of methodology that can predict the course of subsequent degradation and anticipate failure.

There is a paucity of information about the effect of absorbed moisture on the local dynamics in glassy adhesives. Difficulties arise because the time scale of local dynamics in these materials can be as fast as few picoseconds, and an experimental technique operable at high frequency (where fast processes are observed) and adaptable to adhesive joint configuration is needed. Broad-band dielectric relaxation spectroscopy (DRS) is one method that meets those requirements. a rare example of the use of high-frequency DRS to study moisture absorption in adhesive joints is the excellent work of Pethrick and his colleagues [13–15], though the main thrust of their research is aimed at the development of a field-operable non-destructive inspection (NDI) tool based on DRS. It is clear, however, that the success of their efforts hinges upon a thorough understanding of the relevant science and, hence, our approaches are complementary.

The interpretation of DRS data on a molecular level can be greatly aided by the use of a complementary technique capable of providing information in real time about the chemical state of the matter. Of such techniques, Fourier Transform Infrared Spectroscopy (FTIR) represents the most attractive choice because of: (1) the unmatched wealth of the information about the chemical state of the matter contained in the infrared portion of the electromagnetic spectrum, (2) the adaptability of near-IR (NIR) to remote (fiber-optic) *in-situ* real-time application, and (3) the possibility of using NIR for NDI. Although the use of conventional FTIR spectroscopy to detect moisture in polymers has been well documented in the literature [16–21], we are not aware of any study of moisture absorption in adhesive joints by NIR. The combined use of DRS and NIR spectroscopy is designed to afford a simultaneous examination of *physical* (DRS) and *chemical* (FTIR) changes at a molecular level in adhesive joints exposed to an aggressive environment.

It is clear that, in an attempt to answer the questions raised above, any number of combinations of adhesives, substrates, surface treatments and aggressive environments could be selected for investigation. Here, we focus attention on the effect of moisture on the local dynamics of two epoxy-amine adhesive formulations (model and commercial).

THEORETICAL BACKGROUND

In an isotropic amorphous system, with negligible internal field factors, dielectric permittivity is related to the dipole moment correlation function by a Fourier transformation [22]:

$$\frac{\varepsilon^*(\omega) - \varepsilon_\infty}{\varepsilon_0 - \varepsilon_\infty} = 1 - i\omega \int_0^\infty [\exp(-i\omega t)]\Phi(t)dt \tag{1}$$

where ε_0 is the limiting low-frequency value of the dielectric permittivity, ε_∞ is the limiting high-frequency dielectric permittivity, ω is angular frequency, and Φ(t) is the relaxation kernel that can be obtained from the dipole correlation function [23]:

$$\Phi(t) = \frac{\sum_i^N \sum_j^N \langle \mu_i(0)\mu_j(t)\rangle}{\sum_i^N \sum_j^N \langle \mu_i(0)\mu_j(0)\rangle} \tag{2}$$

where μ_i(0) and μ_i(t) denote the elementary dipole moment of a molecule i at time t = 0 and t, respectively. The correlation function expressed in this form takes into account both equilibrium and dynamic angular correlations between molecules. The relaxation kernel, Φ(t), (Eqs. (1) and (2)) is often quantified *via* a stretched exponential function of the Kohlrausch-Williams-Watts [24] (KWW) type:

$$\Phi(t) = Ce^{-(t/\tau)^\beta} \tag{3}$$

where C is a constant, τ is the relaxation time and β is the stretching exponent ranging from 0 to 1. The KWW function is commonly used to describe the (skewed) α process in the isotropic state. The relaxation kernel can be also evaluated from the experimental data. To do that, it is sufficient to use only one portion of the permittivity, real or imaginary, in Eq. (1), since they are related by the Kramers-Kronig transform. For example, by taking the imaginary part of the Fourier transform of Eq. (1) we obtain:

$$\Phi(t) = \frac{2}{\pi} \int_0^\infty \frac{\varepsilon''(\omega)}{\varepsilon_0 - \varepsilon_\infty} \frac{\cos(\omega t)}{\omega} d\omega \tag{4}$$

In our earlier studies, however, instead of transforming the frequency domain dielectric data into the time domain using a discrete Fourier transform, where spectral features may be truncated, we would transform the relaxation kernel, $\Phi(t)$, into the frequency domain, using the technique described by Dishon *et al.* [25] and then fit the experimental data to the transformed kernel with appropriate parameters. alternatively, ε^* may be modeled by a number of empirical functions in the frequency domain; a particularly popular and robust form is the Havriliak-Negami [26] (HN) function given as:

$$\varepsilon^*(\omega) = \varepsilon_\infty + \frac{\varepsilon_0 - \varepsilon_\infty}{[1 + (i\omega\tau_{HN})^a]^b} + i\frac{\sigma}{\omega\varepsilon_v} \tag{5}$$

where a and b are the dispersion shape parameters, σ is the conductivity, ε_v is the vacuum permittivity, and the other parameters are defined in Eq. (1). The HN equation is a generalization of the Cole-Cole (CC) equation, to which it reduces for $b = 1$, and a generalization of the Cole-Davidson (CD) equation, to which it reduces for $a = 1$. HN and CC functional forms were employed in this study to describe local dynamics.

EXPERIMENTAL

Materials

Two multifunctional epoxy-amine formulations were investigated: a model system and a commercial system. The model system consisted of diglycidyl ether of Bisphenol A or DGEBA (Aldrich Chem. Co.) and methylene dianiline or MDA (Aldrich Chem. Co.). The stoichiometric amounts of epoxy groups and amine hydrogen were used and the components were mixed until a clear mixture was obtained. The cure schedule consisted in heating the sample from 20 to 180°C at 5°C/min and maintaining it at 180°C for 30 min. The DSC Tg_∞ was 170°C. The commercial sample investigated was an unsupported epoxy-amine adhesive film (FM73) supplied by Cytec Fiberite. The cure schedule consisted in heating from 20 to 110°C at 5°C/min and maintaining it at 110°C for 60 min. The DSC Tg_∞, was 93°C. Samples were cured between aluminum adherends. The

adherend surface was cleaned with a solvent (acetone) prior to the application of the resin. The bondline thickness was 50 μm. all samples used in this study were fully cured (DSC and FTIR controls were run) and were subjected to an identical thermal history (by heating above the Tg_∞) prior to the exposure to environment, in order to minimize the effect of structural relaxation between different samples. Then, samples were placed in a controlled environment at 60°C and 98% relative humidity (maintained with a saturated $NaHSO_4$ solution) and tested at desired time intervals.

Techniques

The principal experimental technique we have used is broad-band dielectric relaxation spectroscopy (DRS). Of the experimental methods available for the study of relaxation processes in polymeric and molecular glass formers, DRS is rapidly becoming a dominant tool [27, 28]. The great attraction of DRS derives from an unparalleled frequency range available (up to 16 decades) that enables one to conduct fundamental studies of molecular dynamics of condensed matter in various phases and at different temperatures: from amorphous liquids to liquid crystals to an amorphous or crystalline glass; from high temperature, where the dipole relaxation times are of the order of picoseconds, through the vitrification process where relaxation times in the glassy state reach tens to hundreds of seconds. A more detailed description of our experimental facility for dielectric measurements is given elsewhere [29, 30] and several excellent reviews of experimental methodology for dielectric measurements were recently published [31]. However, briefly, we have used a Solartron 1260 Impedance Gain Phase Analyzer (10 μHz–32 MHz) with broad-band dielectric converter (Novocontrol GmBh), Hewlett-Packard (HP) 4284 A Precision LCR Meter (20 Hz–1 MHz), Hewlett-Packard 4291 A RF Impedance Analyzer (1 MHz–1.8 GHz) and Hewlett-Packard 8752A Network Analyzer (300 kHz–1.3 GHz). All instruments are interfaced to computers *via* IEEE 488.2 and are equipped with heating/cooling capabilities, including Novocontrol's Novocool System. A variety of sample cells were employed, including parallel plates, high-precision extension airlines, cells for the simultaneous dielectric/remote fiber optic FTIR tests, *etc.* Supporting evidence was

obtained from Fourier transform infrared (FTIR) spectroscopy, using Nicolet Instrument's Magna 750 Spectrometer [32], and differential scanning calorimetry (DSC), using a Perkin-Elmer model 7 DSC at a heating rate of 10°C/min.

RESULTS AND DISCUSSION

We begin by presenting the results for our model system, composed of the stoichiometric amounts of DGEBA and MDA. This system is miscible and has a calorimetric Tg of -12°C prior to the onset of curing reactions. Dielectric permittivity and loss in the frequency domain (note, 11 decades of frequency) with temperature as a parameter *before* the onset of cure are shown in Figure 1. The solid lines are fits to the HN functional form (Eq. (5)). Since dielectric permittivity and loss are related by the Kramers-Kronig transforms, the remaining figures in the paper contain only the dielectric loss data. The segmental α process and the local β process are clearly observed, in agreement with earlier results for similar systems [33–35]. We reiterate that the uncured system is shown as reference only and all subsequent results pertain to fully-cured networks. A fully-cured DGEBA-MDA network (see Experimental Section) had a calorimetric Tg_∞ of 170°C. Dielectric loss in the frequency domain of a fully-cured sample is shown in Figure 2. In the temperature range of Figure 2 the network is well below its calorimetric Tg_∞ and we observe only the secondary β relaxation. Because of its localized nature, the β process is precisely what we are interested in (we shall not be concerned with the dynamics of the segmental α process in glassy networks). In general, the origin of these β relaxations remains elusive, but appeals have been made in the literature to explanations ranging from far-IR phonon excitations [36] cage-rattling motions [37], a universal glassy state phenomenon [38], and various types of local/side-chain motions [39]. In cured epoxy networks, however, it is generally agreed that the origin of the β process lies in the local motions associated with hydroxyl groups [40]. This interpretation seems to be amply supported by the results of our study, as will be shown later. The β process in Figure 2 is Arrhenius: with decreasing temperature it slows down, broadens and decreases in intensity.

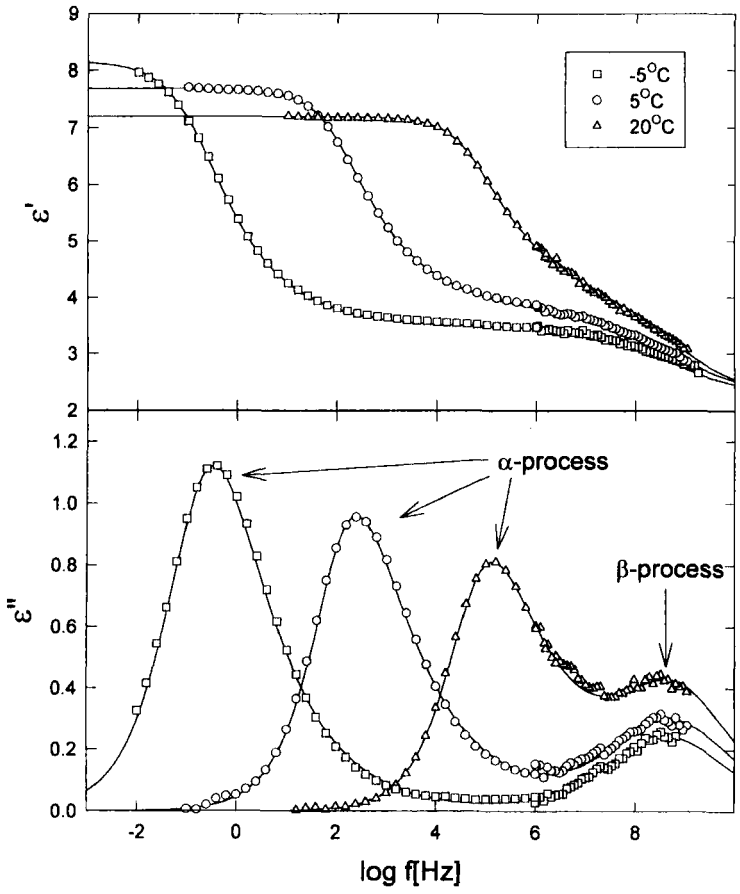

FIGURE 1 Dielectric permittivity and loss in the frequency domain for uncured DGEBA/MDA mixture with temperature as a parameter. Solid lines are fits to Havriliak-Negami equation.

Once the dynamics of the fully-cured dry network were established, we proceeded with a systematic study of the effect of absorbed moisture on the local dynamics. We preface the presentation and discussion of these results with two important comments. First, we stress that we shall not be principally concerned here with the kinetics of moisture absorption. And, second, we acknowledge numerous efforts to monitor moisture absorption quantitatively by tracking dielectric permittivity at an arbitrary frequency [9, 13–15], but hasten

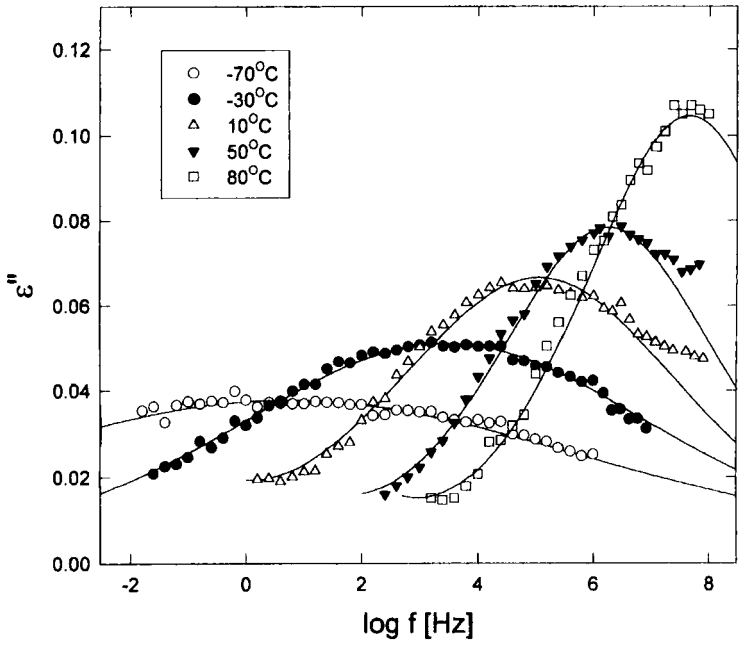

FIGURE 2 Dielectric loss in the frequency domain for fully-cured DGEBA/MDA with temperature as a parameter. Solid lines are fits to Havriliak-Negami equation.

to add that the dielectric response of a changing structure is a function of both exposure time *and* frequency. Therefore, if one is interested in *dynamics*, the correct way to track it is by recording the relaxation spectra at selected times and over a wide frequency range. Because of the local nature of β relaxations, it was anticipated that the dynamics of this process would be particularly sensitive to the absorbed moisture from the very beginning of exposure to environment. In that case, the β process could serve as a molecular indicator of the local dynamics, governed by the interactions between the thermoset network and the absorbed moisture. Figure 3A shows dielectric loss in the frequency domain measured at various temperatures, following a 3-day exposure to 60°C/90%RH. There is practically no change in the average relaxation time (defined as $\tau = 1/2\pi f_{max}$) for the β process after 3 days, in comparison with a dry sample (contrast Figs. 2 and 3). But we do observe an increase in intensity and a clear sign of the emergence of another relaxation, first manifested as a shoulder on the

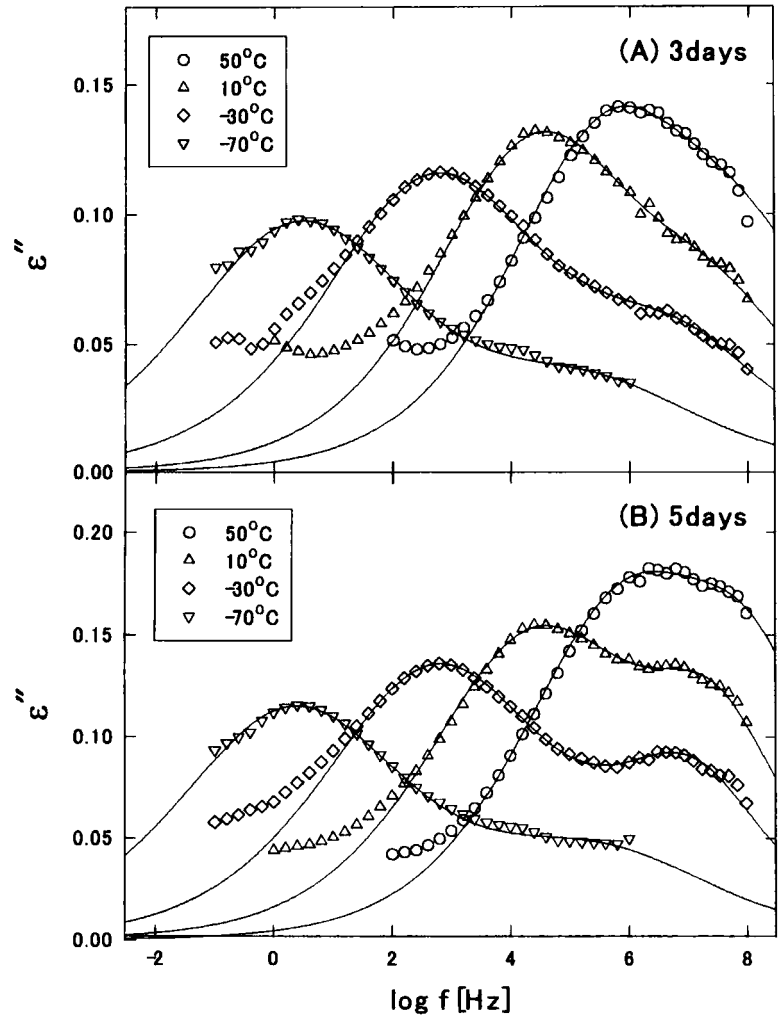

FIGURE 3 Dielectric loss in the frequency domain for fully-cured DGEBA/MDA with temperature as a parameter: A. after 3-day exposure to environment; B. after 5-day exposure to environment. Solid lines are fits to Havriliak-Negami equation.

high-frequency side. This new process, which we term γ, becomes more pronounced after a 5-day exposure, as seen in Figure 3B. A deconvolution of two relaxations was performed and an example is shown in Figure 4; the presence of two processes is beyond doubt and the deconvolution is physically meaningful. Both processes are

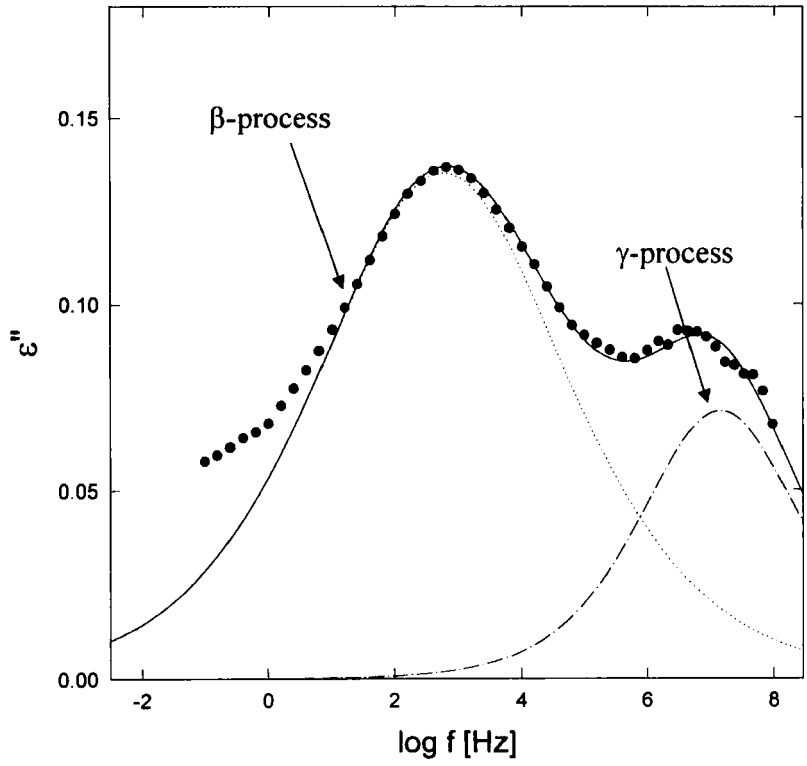

FIGURE 4 Dielectric loss in the frequency domain after 5-day exposure to environment, measured at −30°C. The β and γ processes were fit to the Cole–Cole equation.

symmetric and the solid lines in Figure 4 are fits to the Cole–Cole (CC) equation. An alternative way of displaying the effect of absorbed moisture on the local dynamics is by plotting the dielectric loss in the frequency domain at a constant measuring temperature and with exposure time as a parameter. One such example is presented in Figure 5 (measured at −30°C), which clearly shows the gradual development of β and γ relaxations with increasing exposure time.

The frequency of maximum loss for different relaxation processes is plotted as a function of reciprocal temperature in Figure 6. Both β and γ processes are Arrhenius, with activation energy of 53–57 kJ/mol and 28 kJ/mol, respectively. The β process in the dry sample appears to be a bit faster and to have slightly lower activation energy than the moist samples. The activation energy for the γ process is of

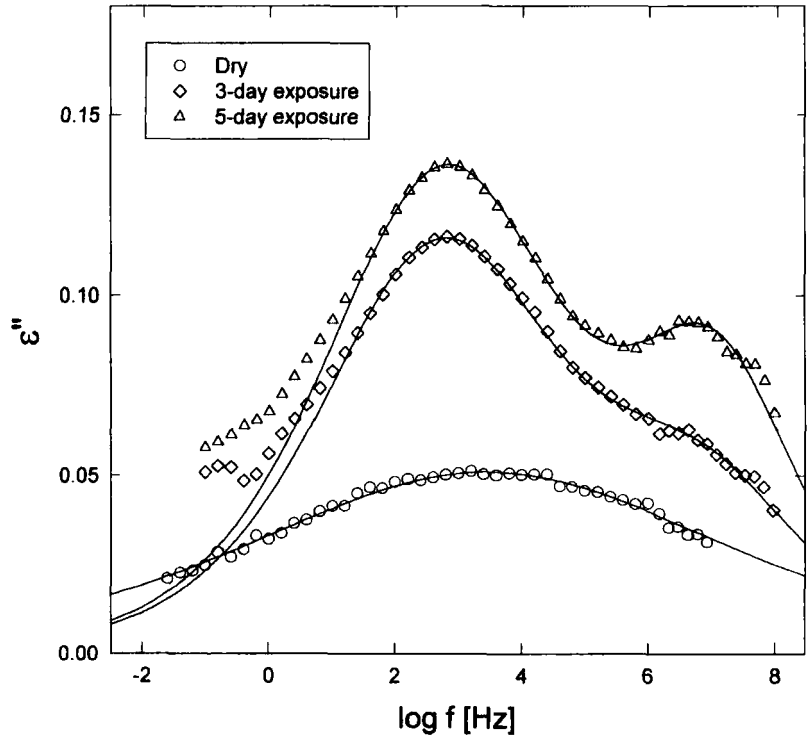

FIGURE 5 Dielectric loss in the frequency for the fully-cured DGEBA/MDA with exposure time as a parameter, measured at −30°C. Solid lines are fits to Havriliak-Negami equation.

the order of magnitude generally observed for the local (Johari-Goldstein [38]) processes in many polymers. The dielectric strength of β and γ processes was found to increase with exposure time and with measuring temperature.

An important question is what are DRS data telling us about the molecular origin of β and γ relaxations? First, it is evident that the dynamics of the β process change with absorbed moisture. The initial relaxations associated with hydroxyl groups are slowed down (by about one-half a decade with respect to the dry sample) through the interactions between the network and a portion of the absorbed water molecules. The precise nature of these interactions will be discussed further with the results of FTIR measurements. The faster γ process is due to the other portion of the absorbed water molecules (that are not engaged in water-network interactions) although it is also not

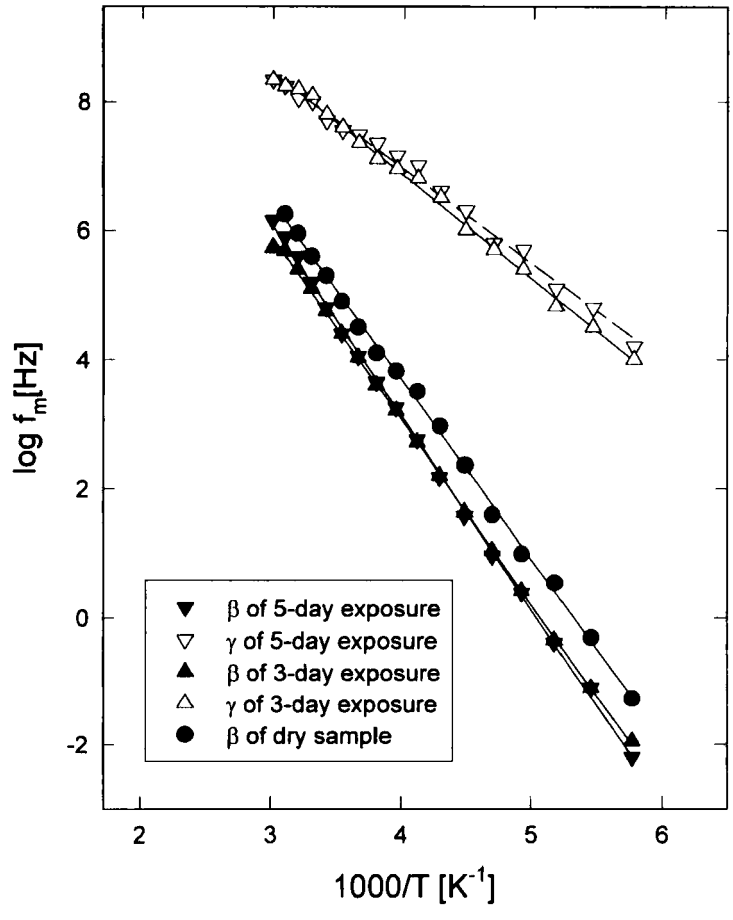

FIGURE 6 Frequency of dielectric loss maximum, f_m, as a function of reciprocal temperature for dry, and moist DGEBA/MDA.

immediately clear from DRS data in what form (isolated single molecules, dimers, trimers) water resides within the adhesive. In comparison with liquid water, which at 20°C has a dielectric loss peak at about 20 GHz (corresponding to an average relaxation time of about 9 picoseconds) [41], the relaxation time of the γ process is longer by more than a decade on the frequency scale. Whether the reason for this is physical (*e.g.*, steric hindrance due to neighboring benzene rings) or chemical (*e.g.*, some weak interactions with network groups), is not apparent from the DRS data. The average relaxation time of the γ process at 20°C is of the order of 1,000 ps. Interestingly, this is in

agreement with the value of 700 ps reported by Jelinski *et al.*, in their study of water in DGEBA/m-MDA networks by solid state NMR spectroscopy [42]. That time (700 ps) was described as the average residence time of a water molecule at one site before it hops to another site. These authors also argue that "free" water (defined as isotropically-mobile with the same relaxation time as liquid water) is not present. Strictly speaking this is true, though our FTIR evidence (offered below) suggests that non hydrogen-bonded water exists as isolated molecules whose dynamics are slightly slowed down by steric hindrance. More about the size and form of the interactions that underlie the γ process will be said in conjunction with the results of FTIR measurements and molecular simulation studies.

The fully-cured FM73 commercial adhesive (see Experimental Section) had a calorimetric Tg_∞ of 93°C. Dielectric loss in the frequency domain with temperature as a parameter for this sample is shown in Figure 7. With decreasing temperature the β process slows

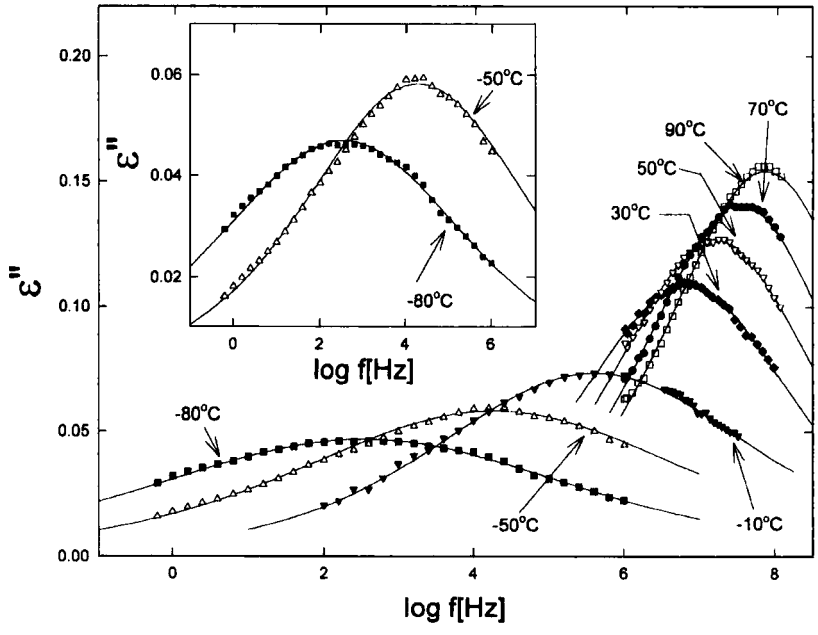

FIGURE 7 Dielectric loss in the frequency domain for fully-cured FM73U with temperature as a parameter. Solid lines are fits to Havriliak-Negami equation.

down and broadens, displaying a response similar to that of the model system. The loss spectrum for the β process in the dry sample is also symmetric and the solid lines in Figure 7 represent fits to the CC equation. In Figure 8 we show the loss data measured at 25°C after 2, 4 and 8 hours of exposure to environment. The average relaxation time (see the location of f_{max}) increases slightly within the first two hours and then levels off, while the loss intensity continues to increase. The shape of the spectrum, however, remains symmetric and the solid lines in Figure 8 are CC fits. But after a 10-day exposure there was one noticeable difference; the spectra were asymmetric and were described by the HN functional form (Fig. 9). The asymmetric shape of the spectrum is not typical of the β process and we interpret it as a consequence of the overlap of β and γ relaxations. Although we did not observe a separate γ process, its presence is strongly supported by

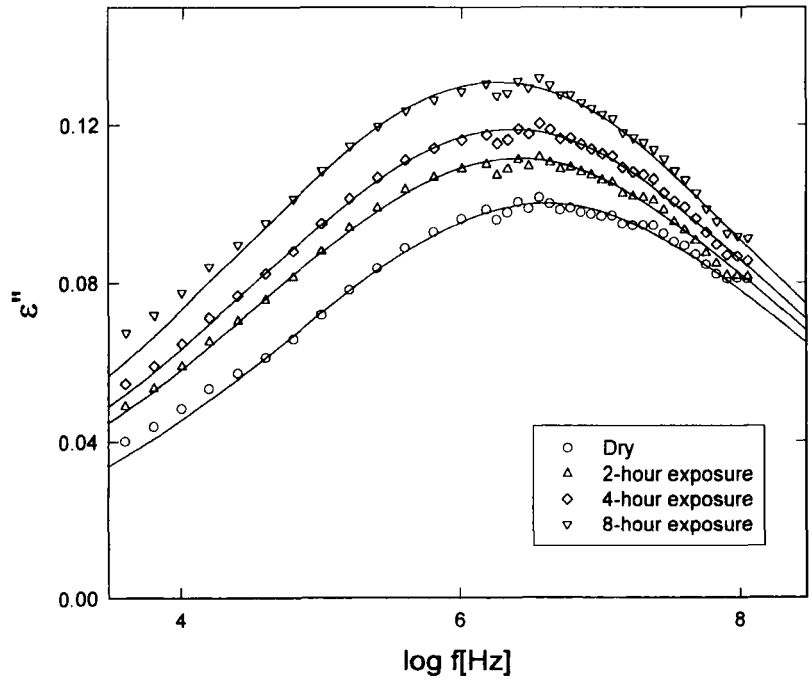

FIGURE 8 Dielectric loss in the frequency domain for cured FM73U with exposure time as a parameter. Solid lines are fits to Havriliak-Negami equation.

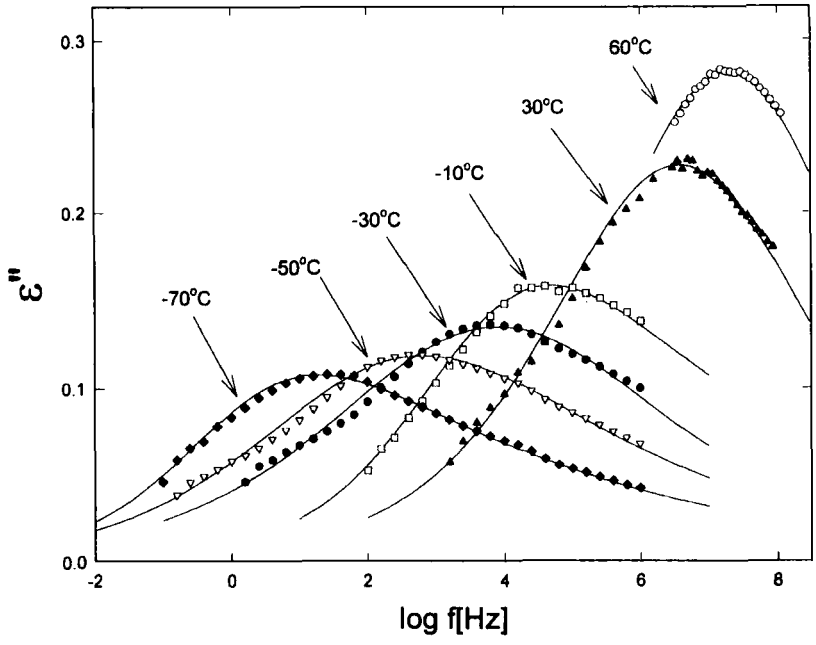

FIGURE 9 Dielectric loss in the frequency domain for FM73U after 10-day exposure, with temperature as a parameter. Solid lines are fits to Havriliak-Negami equation.

a broad high-frequency tail that is particularly evident in the low-temperature spectra. The fact that we do not see a separate γ process, as in the model system, is not necessarily surprising considering a difference in the chemical composition between these two formulations. We made no attempts at deconvolution of spectra in Figure 9 (because the result would have little physical justification) and have continued to treat this relaxation as one (β) process (while aware of possible drawbacks). An alternative view of the effect of absorbed moisture on the β dynamics is depicted in Figure 10, which shows dielectric loss in the frequency domain with exposure time as a parameter, measured at 60°C. Solid lines in this figure are HN fits. Several important observations are made in this figure. First, note that the average relaxation time ($\tau = 1/2\pi f_{max}$) for the β process at temperatures above *ca.* 25°C is of the order of nanoseconds or less and, hence, its detection hinges on the ability to conduct high-precision dielectric measurements in the frequency range above

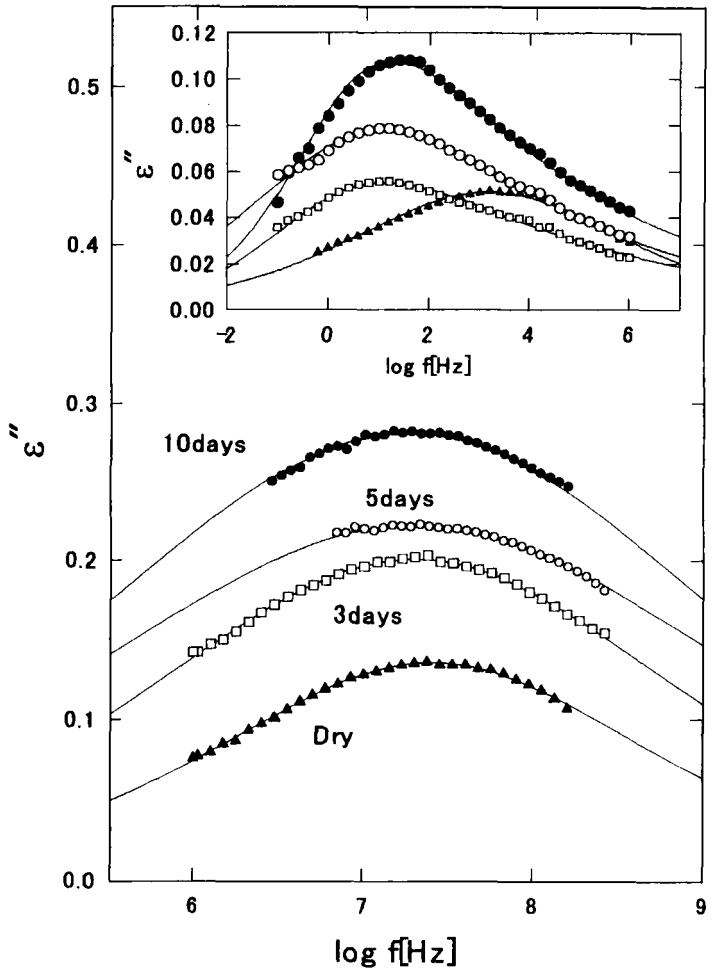

FIGURE 10 Dielectric loss in the frequency domain for FM73U with exposure time as a parameter, measured at 60°C. Solid lines are fits to Havriliak-Negami equation. Inset: dielectric loss measured at −70°C.

1 MHz. This is an important consideration in the ongoing efforts aimed at the implementation of DRS as an NDI tool for adhesive joints. Further, it is interesting to note that while the loss peak intensity increases with exposure time, the average relaxation time measured at 60°C remains largely unaffected by the absorbed moisture. But as the measuring temperature is decreased, we observe

a progressive divergence in the average relaxation time for dry and moist samples, as evidenced by data in the inset in Figure 10 (measured at $-70°C$). This divergence is perhaps best seen in the composite plot of frequency of maximum loss as a function of reciprocal temperature, shown in Figure 11. Note that both processes are Arrhenius, with activation energy of 41 kJ/mol and 60 kJ/mol for dry and moist samples, respectively. Finally, we note that the β dynamics were reversible upon moisture desorption.

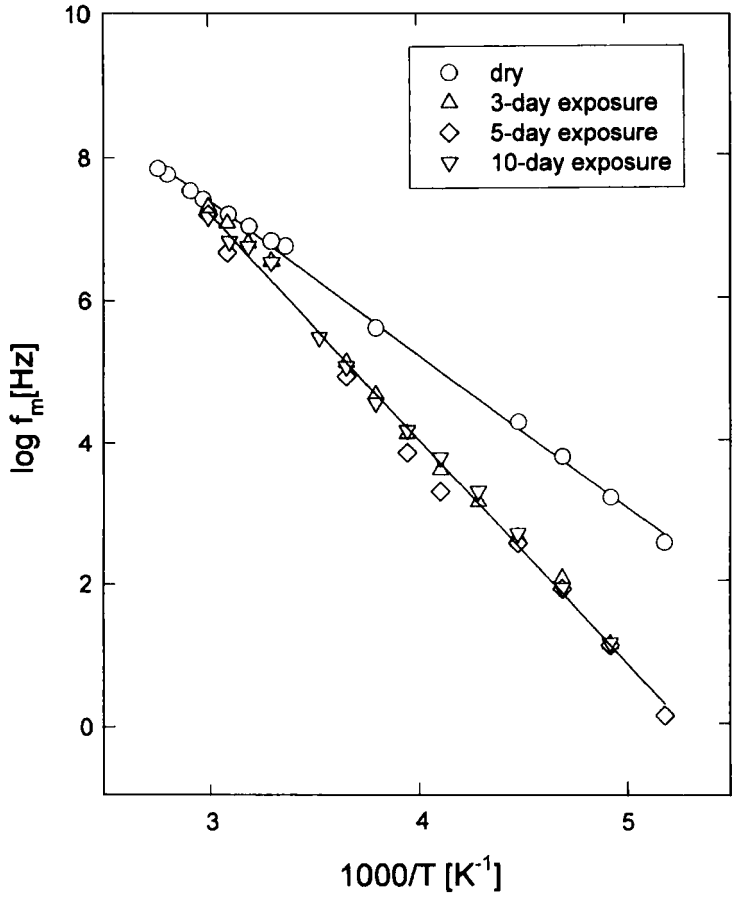

FIGURE 11 Frequency of dielectric loss maximum, f_m, as a function of reciprocal temperature for dry and moist FM73U.

Next, we present and discuss the results of near-IR (NIR) and mid-IR (MIR) analysis of the model (DGEBA/MDA) system. The NIR spectra of dry and moist (fully-cured) DGEBA/MDA networks are contrasted in Figure 12. All major peaks of relevance in epoxy/amine systems are present: epoxy absorption at 4530 and 6080 cm^{-1}, amine

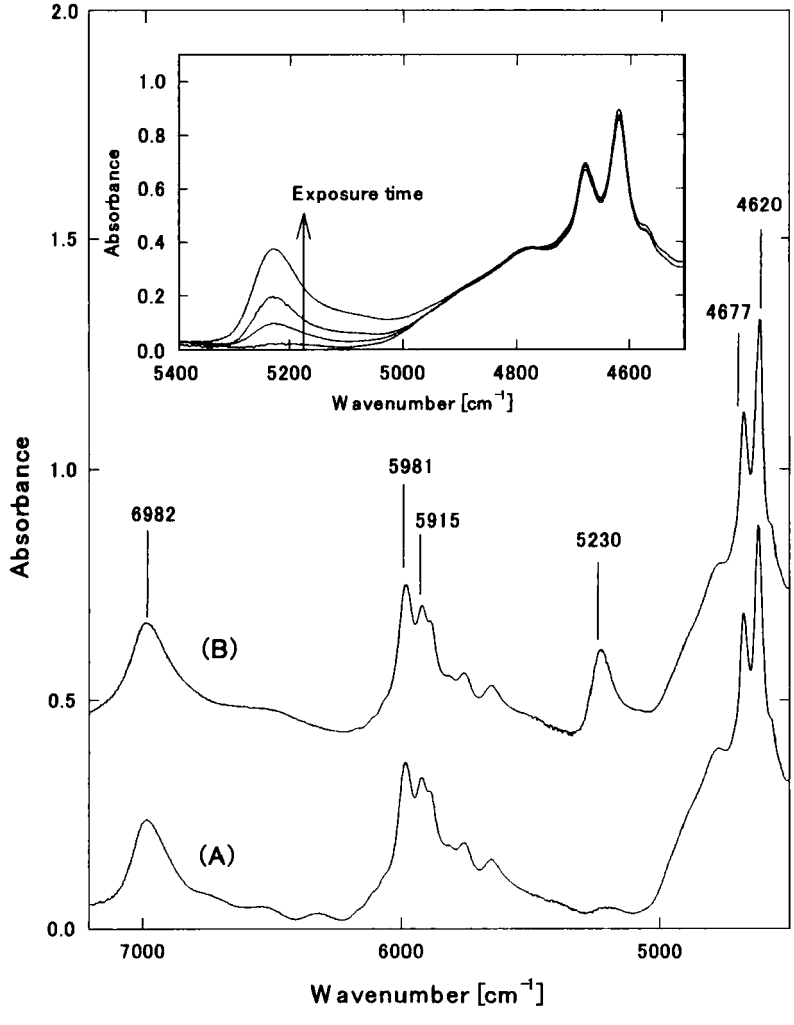

FIGURE 12 Near-IR spectra of DGEBA/MDA: (A) dry and (B) after 1-day exposure. Inset: series of spectra at different exposure times: dry, 2 hours, 1 day, 13 days.

absorption at 5056 and 6670 cm^{-1}, and hydroxyl absorption at 4800–4900 cm^{-1} and 7000 cm^{-1}. A comprehensive identification of the NIR spectra of epoxy networks before, during and after cure is given elsewhere [43]; here we focus attention on the peak at 5210 cm^{-1}, which is associated with the absorbed moisture. The observed spectral difference in Figure 12 establishes this peak as the indicator of absorbed moisture. A sequence of NIR spectra taken at selected time intervals during environmental exposure is shown in the inset in Figure 12. An increase in the absorption intensity is evident: careful inspection of the data also reveals a consistent increase in the absorption intensity at the lower wavenumber side of the 5210 cm^{-1} peak, suggesting a gradual development of another absorption mechanism. This is an interesting finding. A deconvolution of the broad absorption was carried out and two absorption peaks were clearly detected, as seen in Figure 13. These two peaks were centered at 5230 and 5137 cm^{-1}, respectively, and were both Gaussian. The absorption intensity of each peak is a linear function of absorbed moisture. But, because the absorption in this range is associated with a combination of bending (1600–1650 cm^{-1}) and stretching (3100–3800 cm^{-1}) vibrations, we made no further attempts at identifying these peaks with specific interactions. In an excellent recent study of water absorption in a tetrafunctional epoxy/amine (TGDDM/DDS) network by NIR, Musto *et al.* [20, 21] were able to deconvolute the broad absorption at around 7000 cm^{-1} into three distinct components centered at 7075, 6820 and 6535 cm^{-1}, respectively. These peaks were associated with isolated single water molecules (7075), water molecules hydrogen-bonded to one site (6820) and water molecules hydrogen-bonded to two sites (6535). An important finding in their study was that each water molecule interacts with two proton acceptors. We were hesitant to deconvolute the absorption peak around 7000 cm^{-1} in our networks because of insufficiently high resolution.

The MIR spectra of a sample exposed to moisture for times ranging from 10 minutes to 8 days are shown in Figure 14. Of major interest here is the range between about 3100 and 3800 cm^{-1}, where vibrational modes due to various forms of hydrogen bonding are located. Normalization of spectra with respect to absorption due to the phenyl group (at 3035 cm^{-1}) and alkyl groups (at 2963, 2930 and 2872 cm^{-1}) enables one to track the change in the absorption intensity

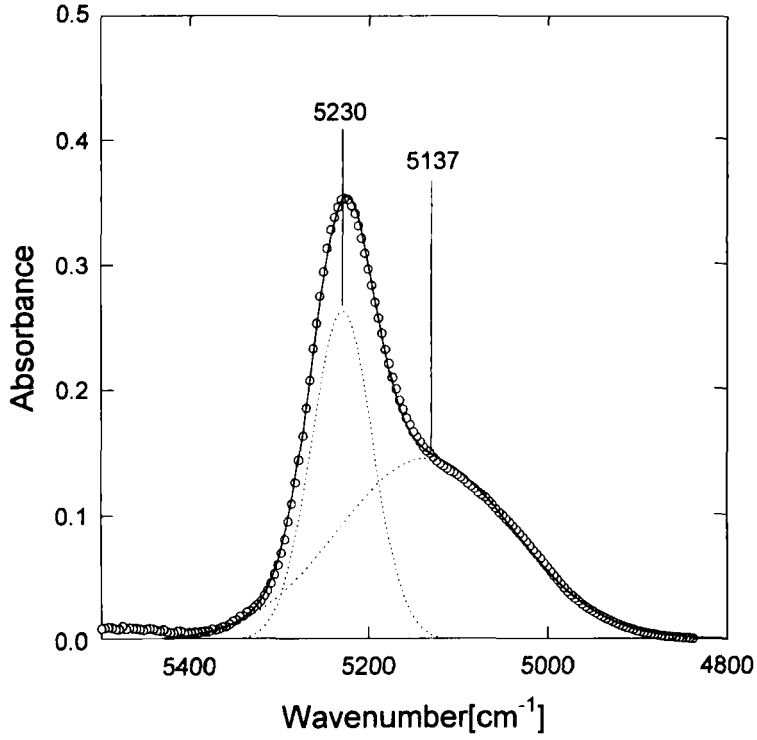

FIGURE 13 Deconvolution of the 5400–4800 cm^{-1} range after 13-day exposure. Two separate processes were described by Gaussian function.

in the range between 3100 and 3800 cm^{-1} as a function of exposure time. This is clearly seen in Figure 14. A further insight into the progressive effect of absorbed moisture is obtained by subtracting the spectrum of a dry sample from that of each moist sample. The resulting spectra are shown in Figure 15 and two distinct regions are observed: a sharp absorption around 3600 cm^{-1} and a broad and asymmetric absorption between about 3600 and 3100 cm^{-1}. The intensity of both absorptions increases with increasing exposure time. The question is what is the origin of these absorption peaks? First, we consider the narrow absorption at high wavenumber that was fit to a Gaussian function with a peak at 3626 cm^{-1} (see Fig. 16). This absorption has been observed in a number of systems with low water concentration, ranging from polymer networks [20, 21] to mixtures of water and a non-polar solvent (*e.g.*, CCl_4) [44–46], and has been

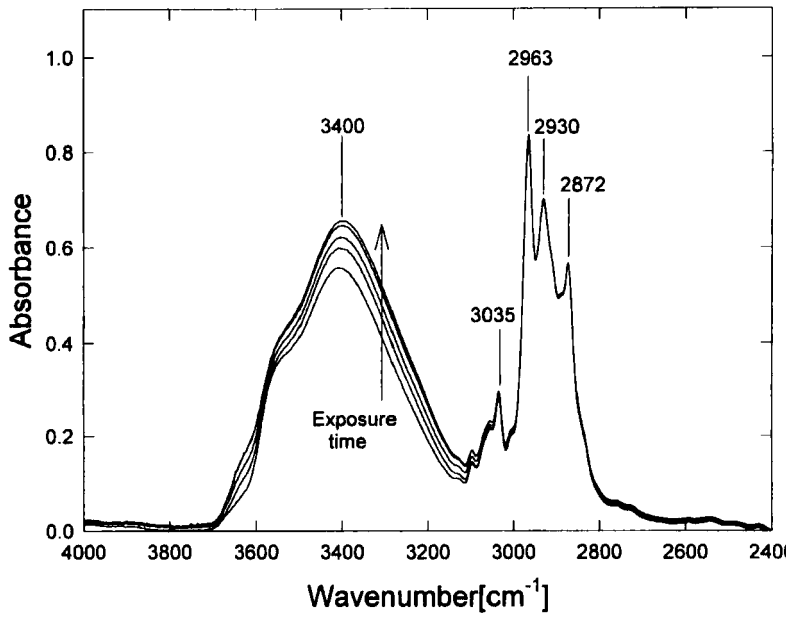

FIGURE 14 Mid-IR spectra for DGEBA/MDA at different exposure times: dry, 10 minutes, 1 hour, 1 day, and 8 days.

associated with non-hydrogen-bonded water. In our epoxy-amine network, this absorption is assigned to water molecules located in the pockets surrounded by hydrophobic moieties, such as benzene rings, where the likelihood of hydrogen bonding is low. Based on the MIR data, the non hydrogen-bonded water accounts for about 13% of the total absorbed water. The ability to measure precisely the concentration of a dipole group raises interesting possibilities as regards the correlation between vibrational and dielectric spectroscopy. Recall that non-hydrogen-bonded water, that gives rise to a MIR absorption peak centered at $3626\,cm^{-1}$, is also proposed to be at the origin of the dynamic γ process. This, in effect, provides a link between chemical (measured by FTIR) and physical (measured by DRS) phenomena that accompany water absorption into the network. For example, a correlation could be sought between the concentration of dipoles extracted from FTIR spectra and the dielectric strength of a relaxation process (*e.g.*, β or γ) *via* the Kirkwood-Frohlich equation.

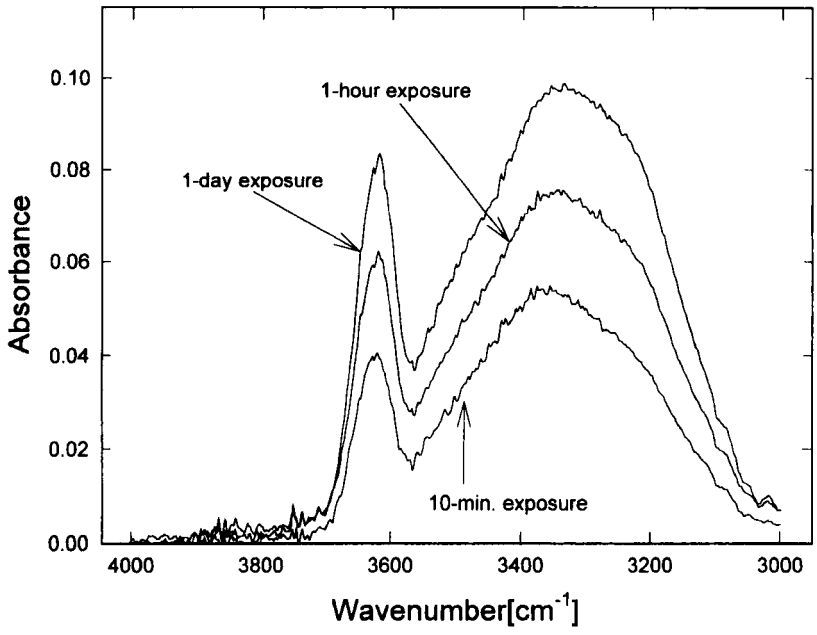

FIGURE 15 Mid-IR difference spectra for DGEBA/JMDA at different exposure times: 10 minutes, 1 hour, and 1 day.

We next proceeded with attempts to deconvolute the broad absorption range between 3600 and 3100 cm^{-1}. The best results were obtained using three Gaussian functions, as shown in Figure 16, with peaks at 3523, 3380 and 3210 cm^{-1}. The intensity of each absorption (as defined by the area under the absorption peak) increases with increasing exposure time. But when each absorption intensity is normalized with respect to the total intensity, we observe an increase in the absorption at 3210 cm^{-1}, a decrease at 3380 cm^{-1}, and little change at 3523 and 3626 cm^{-1}. The presence of several absorption peaks tells us two things: 1) the absorption mechanism is more complex than originally thought, and 2) the concept of two types of absorbed moisture, often lumped under "loosely" and "strongly" bound, is an oversimplification of the actual situation. But what can we say about the molecular origin of absorption at 3523, 3380 and 3210 cm^{-1}? For one, the hydrogen-bonded water accounts for approximately 87% of the total water absorbed in the network. We note that this number is considerably higher than the values between

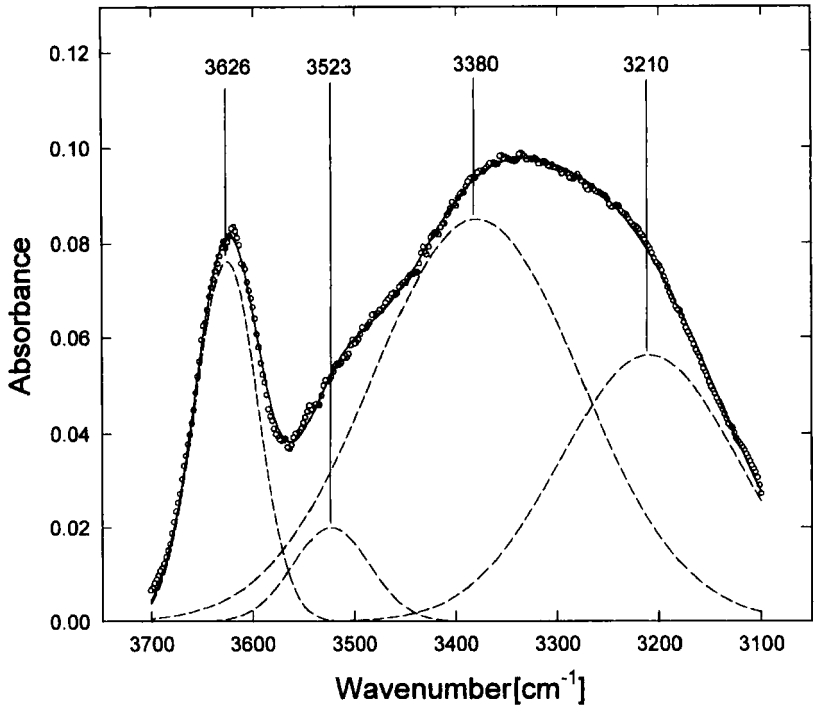

FIGURE 16 Deconvolution of difference spectra in the range of 3700–3100 cm^{-1} after 1-day exposure. Each peak was described by a Gaussian function.

60 and 40% reported by other investigators [14,21]. Further, it is known that the intensity of hydrogen bonding increases with decreasing wavenumber, *i.e.*, from 3523 to 3210 cm^{-1} in our case. We have also observed an increase in the intensity of absorption peaks at 3380 and 3210 cm^{-1} during environmental exposure, as evidenced by a shift to lower frequency by about 40 and 50 cm^{-1}, respectively. But the identification of each absorption peak with a specific type of hydrogen bond is not straightforward. In a DGEBA/MDA network, absorbed water can form a hydrogen bond with a number of sites on the network, including the ether oxygen, the hydroxyl group and the tertiary amine nitrogen.

Moreover, the same water molecule can participate in one or two hydrogen bonds (with two proton acceptors) when a favorable steric configuration is encountered. Naturally, if the absorbed water forms dimers or trimers, there will also be a possibility of hydrogen bonding

between the adjacent water molecules. The last scenario brings up an interesting question: how large are the absorbed water entities? In an attempt to answer this important question we performed a dynamics simulation study with the aid of a commercial software package Cerius2. A stoichiometric DGEBA/MDA composed of twenty-six molecules of DGEBA and thirteen molecules of MDA was constructed. Nine molecules of water were introduced into the network, bringing the water content to about 1.6% by weight (a reasonable value considering that the maximum water content at the conditions of this study was *ca.* 3% by weight). The molecules were annealed until the total energy reached a minimum value and the simulation was conducted at 300°K. The positions of atoms were calculated at 0.001 picosecond intervals and this was repeated 1,000 times in the course of simulation. Although our simulation was limited to a relatively small network, important observations were made. First, fluctuations involving network atoms and water molecules were detected. But, most importantly, the absorbed water molecules were always separate and no dimers or trimers were observed. Apparently, the available space in the fully-cured networks is too small to accommodate larger structures. Simulation has also revealed that a water molecule participates in hydrogen bonding to only one site on the network, in contrast to the experimental results reported elsewhere. It is clear that a simulation study on a larger network would be useful in this context.

A final comment regards our current efforts aimed at the development of fundamental quantitative correlation between FTIR and DRS data. Specifically, we are seeking to correlate a dielectric material parameter (such as the average relaxation time, dielectric strength or a shape parameter of the dielectric spectrum) with a fundamental parameter deduced from the FTIR spectra (*e.g.*, absorption strength, group concentration). This will be the subject of a forthcoming publication.

CONCLUSIONS

The results presented here provide new insight into the local molecular dynamics and interactions of epoxy/amine networks with water. A smaller portion of the absorbed water does not form hydrogen bonds

with the network. The probable cause for that is steric hindrance imparted by the surrounding network. Molecular dynamics simulation indicates that water is absorbed in the form of isolated single molecules; no evidence of dimers or trimers was found. These water molecules also contribute to a dynamic γ process with activation energy of about 28 kJ/mol. The average relaxation time of the γ process at 20°C is more than an order of magnitude longer than that of liquid water because of the steric factors.

A larger part of absorbed water interacts with various sites on the network that include the ether oxygen, the hydroxyl group and the tertiary amine nitrogen. Deconvolution of absorption peaks in NIR and MIR spectra was performed successfully, but the identification of each absorption with a specific type of water-network interaction is not straightforward and more should be learned before such assignments are made. The water-network interactions also have an effect on the local β dynamics. In the dry sample, the β process is associated with the localized motions of hydroxyl groups. The initial β relaxation is slowed down by almost a decade through the interactions of the absorbed water with the network, while the relaxation spectrum broadens with decreasing temperature. One particularly important finding is that the average relaxation time for the β process at temperatures above 25°C is of the order of nanoseconds or less and, hence, its detection hinges on the ability to perform high-precision dielectric measurements in the frequency range above 1 MHz. This is an important consideration in the ongoing efforts aimed at the implementation of DRS as non-destructive inspection tool for adhesive joints.

Acknowledgement

This material is based on work supported by the AFOSR, Polymer Matrix Composites Program (Dr. Charles Y.-C. Lee, Director).

References

[1] The most recent discussion meeting on this subject was held during the Annual Review of the AFOSR Polymer Matrix Composites Program (Dr. Charles Y.-C. Lee, Director), Long Beach, CA, May 19–20, 2000.
[2] Gledhill, R. A. and Kinloch, A. J., *J. Adhesion* **6**, 315 (1974).
[3] Browning, C. E., *Polym. Eng. Sci.* **18**, 16 (1978).

[4] Keenan, J. D., Seferis, J. C. and Quinlivan, J. T., *J. Appl. Polym. Sci.* **24**, 2375–2387 (1979).
[5] Rowland, S. P. Ed., *Water in Polymers* (ACS Symposium Series 127, American Chemical Society, Washington, DC, 1980).
[6] Sedlacek, B. and Kahovec, J. Eds., *Crosslinked Epoxies* (Walter de Gruyter, Berlin, 1987).
[7] Kaelble, D. H., Moacanin, J. and Gupta, A., In: *Epoxy Resins Chemistry and Technology*, May, C. A. Ed. (Marcel Dekker, New York, 1988), Chap. 6, p. 603.
[8] Apicella, A., In: *International Encyclopedia of Composites*, Lee, S. M. Ed. (VCH Publishers, New York, 1990) **2**.
[9] Nairn, B. J., Dickstein, P. A., Plausinis, D. J. and Spelt, J. K., *J. Adhesion* **48**, 121–136 (1995).
[10] de Neve, B. and Shanahan, M. E. R., *J. Adhesion* **49**, 165–176 (1995).
[11] Maggana, C. and Pissis, P., *J. Polym. Sci. Part B: Polym. Phys.* **37**, 1165–1182 (1999).
[12] Soles, C. L., Chang, F. T., Gidley, D. W. and Yee, A. F., *J. Polym. Sci. Part B: Polym. Phys.* **38**, 776–791 (2000).
[13] Li, Z.-C., Hayward, D., Gilmore, R. and Pethrick, R. A., *J. Mater. Sci.* **32**, 879–886 (1997).
[14] Grave, C., McEwan, I. and Pethrick, R. A., *J. Appl. Polym. Sci.* **69**, 2369–2376 (1998).
[15] Affrossman, S., Banks, W. M., Hayward, D. and Pethrick, R. A., *Proc. Inst. Mech. Eng.* **214**, Part C, 87–102 (2000).
[16] Antoon, M. K., Koenig, J. L. and Serafini, T., *J. Polym. Sci., Polym. Phys.* **19**, 1567–1575 (1981).
[17] Skrovanek, D. J., Painter, P. C. and Coleman, M. M., *Macromolecules* **19**, 699–705 (1986).
[18] Ngono, Y., Marechal, Y. and Mermilliod, N., *J. Phys. Chem. B* **103**, 4979–4985 (1999).
[19] Ngono, Y. and Marechal, Y., *J. Polym. Sci. B: Polym. Phys.* **38**, 329–340 (2000).
[20] Musto, P., Mascia, L., Ragosta, G., Scarinzi, G. and Villano, P., *Polymer* **41**, 565–574 (2000).
[21] Musto, P., Ragosta, G. and Mascia, L., *Chem. Mater.* **12**, 1331–1341 (2000).
[22] Williams, G., Dielectric Properties, In: *Comprehensive Polymer Science*, Allen, G., Bevington, J. C. Eds. (Pergamon, Oxford, 1989) **2**, Chap. 7, 601–632.
[23] Williams, G., "Molecular Aspects of Multiple Dielectric Relaxation Processes in Solid Polymers" In: *Advances in Polymer Science*, Cantow, H.-J. *et al.* Eds. (Springer-Verlag, Berlin, 1979) **33**, 59–92.
[24] Williams, G. and Watts, D. C., *Trans. Faraday Soc.* **66**, 80 (1970).
[25] Dishon, M., Weiss, G. H. and Bendler, J. T., *J. Res. Natl. Bur. Stand* **90**, 27 (1985).
[26] Havriliak, S. Jr. and Negami, S., *Polymer* **8**, 161 (1967).
[27] Williams, G., "Theory of Dielectric Properties", In: *Dielectric Spectroscopy of Polymeric Materials*, Runt, J. P. and Fitzgerald, J. J. Eds. (American Chemical Society, Washington, DC, 1997), Chap. 1, pp. 3–65.
[28] Williams, G., In: *Keynote Lectures in Selected Topics of Polymer Science*, Riande, E., Ed. (CSIC, Madrid, 1997), Chap. 1, pp. 1–40.
[29] Fitz, B., Andjelic, S. and Mijovic, J., *Macromolecules* **30**, 5227–5238 (1997).
[30] Andjelic, S., Fitz, B. and Mijovic, J., *Macromolecules* **30**, 5239–5248 (1997).
[31] Kremer, F. and Arndt, M., "Broadband Dielectric Measurement Techniques", In: *Dielectric Spectroscopy of Polymeric Materials*, Runt, J. P. and Fitzgerald, J. J. Eds. (American Chemical Society, Washington, DC, 1997), Chap. 5, p. 139.
[32] Mijovic, J. and Andjelic, S., *Macromolecules* **29**, 239–246 (1996).
[33] Casalini, R., Corezzi, S., Fioretto, D, Livi, A. and Rolla, P. A., *Chem. Phys. Lett.* **258**, 470 (1996).

[34] Corezzi, S., Capaccioli, S., Gallone, G., Livi, A. and Rolla, P. A., *J. Phys.: Condens. Matter* **9**, 6199 (1997).
[35] Fitz, B. D. and Mijovic, J., *Macromolecules* **32**, 4134–4140 (1999).
[36] Angell, C. A., Boehm, L., Oguni, M. and Smith, D. L., *J. Mol. Liq.* **56**, 275 (1993).
[37] Lewis, L. J. and Wahnstrom, G., *Phys. Rev. E* **50**, 3865 (1994).
[38] Johari, G. P. and Goldstein, M., *J. Chem. Phys.* **53**, 2372 (1970).
[39] Meier, G., Fujara, F. and Petry, W., *Macromolecules* **22**, 4421 (1989).
[40] Andjelic, S. and Mijovic, J., *Macromolecules* **31**, 8463–8473 (1997).
[41] Barthel, J., Bachuber, K., Buchner, R. and Hetzenauer, H., *Chem. Phys. Lett.* **195**, 369–373 (1990).
[42] Jelinski, L. W., Dumais, J. J., Cholli, A. L., Ellis, T. S. and Karasz, F. E., *Macromolecules* **18**, 1091–1095 (1985).
[43] Mijovic, J. and Andjelic, S., *Macromolecules* **28**, 2787–2796 (1995).
[44] Harris, D. C. and Bertolucci, M. D., *Symmetry and Spectroscopy* (Dover Publications, New York, 1989), Chap. 3, pp. 93–224.
[45] Luck, W. A. P., "Infrared Studies of Hydrogen Bonding in Pure Liquids and Solution", In: *Water, A Comprehensive Treaties*, Franks, F. Ed. (Plenum Press, New York, 1973), **2**, Chap. 4.
[46] Gragson, D. E. and Richmond, G. L., *J. Phys. Chem. B* **102**, 569–576 (1998).